

The Role of Rheology in Polymer Extrusion

John Vlachopoulos
Department of Chemical Engineering
McMaster University
Hamilton, Ontario, Canada
E-mail: vlachopj@mcmaster.ca

David Strutt
Polydynamics, Inc.
Hamilton, Ontario, Canada

1.0 Rheology

Rheology is the science of deformation and flow of materials [1]. The Society of Rheology's Greek motto "*Panta Rei*" translates as "All things flow." Actually, all materials do flow, given sufficient time. What makes polymeric materials interesting in this context is the fact that their time constants for flow are of the same order of magnitude as their processing times for extrusion, injection molding and blow molding. In very short processing times, the polymer may behave as a solid, while in long processing times the material may behave as a fluid. This dual nature (fluid-solid) is referred to as *viscoelastic* behavior.

1.1 Viscosity and Melt Flow Index

Viscosity is the most important flow property. It represents the resistance to flow. Strictly speaking, it is the resistance to shearing, i.e., flow of imaginary slices of a fluid like the motion of a deck of cards. Referring to Figure 1.1, we can define viscosity as the ratio of the imposed *shear stress* (force F, applied tangentially, divided by the area A), and the shear rate (velocity V, divided by the gap h)

$$\eta = \frac{\text{SHEAR STRESS}}{\text{SHEAR RATE}} = \frac{F/A}{V/h} = \frac{\tau}{\dot{\gamma}} \quad (1.1)$$

The Greek letters τ (tau) and $\dot{\gamma}$ (gamma dot) are conventionally used to designate the shear stress and shear rate, respectively.

For flow through a round tube or between two flat plates, the shear stress varies linearly from zero along the central axis to a maximum value along the wall. The shear rate varies nonlinearly from zero along the central axis to a maximum along the wall. The velocity profile is quasi-parabolic with a maximum at the plane of symmetry and zero at the wall as shown in Figure 1.2, for flow between two flat plates.

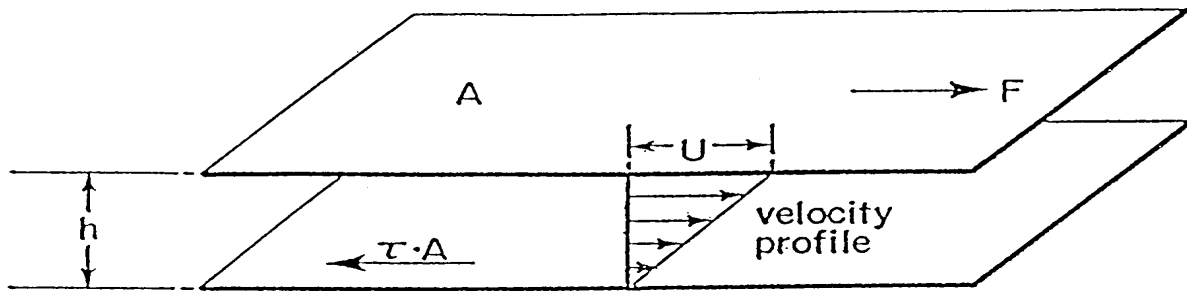


Figure 1.1. Simple shear flow.

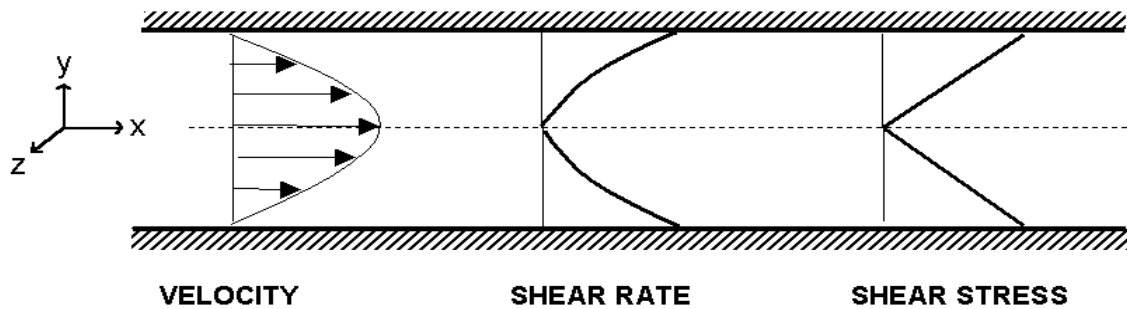


Figure 1.2. Velocity, shear rate and shear stress profiles for flow between two flat plates.

The viscosity in SI is reported in units of Pa·s (Pascal-second). Before the introduction of SI, poise was the most frequently used unit (1 Pa·s = 10 poise). Here are some other useful conversion factors.

$$1 \text{ Pa}\cdot\text{s} = 1.45 \times 10^{-4} \text{ lb}_f \text{ s}/\text{in}^2 = 0.67197 \text{ lb}_m/\text{s ft} = 2.0886 \times 10^{-2} \text{ lb}_f \text{ s}/\text{ft}^2$$

The viscosity of water is 10^{-3} Pa·s while the viscosity of most polymer melts under extrusion conditions may vary from 10^2 Pa·s to 10^5 Pa·s. The shear stress is measured in units of Pa = (N/m²) or psi (pounds (lb_f) per square inch) and the shear rate in reciprocal seconds (s⁻¹).

One remarkable property of polymeric liquids is their *shear-thinning* behavior (also known as pseudo-plastic behavior). If we increase the rate of shearing (i.e., extrude faster through a die), the viscosity becomes smaller, as shown in Figure 1.3. This reduction of viscosity is due to molecular alignments and disentanglements of the long polymer chains. As one author said in a recent article: "polymers love shear." The higher the shear rate, the easier it is to force polymers to flow through dies and process equipment. During single-screw extrusion, shear rates may reach 200 s⁻¹ in the screw channel near the barrel wall, and much higher between the flight tips and the barrel. At the lip of the die the shear rate can be as high as 1000 s⁻¹. Low shear rate on a die wall implies slow movement of the polymer melt over the metal surface. Some die designers try to design dies for cast film or blown film operations not having wall shear rates less than, say 10 s⁻¹, to prevent potential hang-ups of the molten material. When the wall shear stress exceeds 0.14 MPa, sharkskin (i.e. surface mattness) occurs in capillary viscometer measurements using various HDPE grades. At very high shear rates, a flow instability known as melt fracture occurs [2, 3].

Melt Index (MI), Melt Flow Index (MFI), or Melt Flow Rate (MFR) (for polypropylene) refers to the grams per 10 minutes pushed out of a die of prescribed dimensions according to an ASTM Standard [4] under the action of a specified load as shown in Figure 1.4. For PE (ASTM D-1238) the load is 2.16 kg and the die dimensions are D = 2.095 mm and L = 8 mm. The experiment is carried out at 190°C. For the PP, the same load and die dimensions are used, but the experiment is carried out at 230°C.

Under the conditions of melt index measurement with a 2.16 kg load, the wall shear stress can be calculated to be $\tau_w = 1.94 \times 10^4$ Pa (= 2.814 psi) and the wall shear rate approximately $\dot{\gamma} = (1838/\rho) \times \text{MI}$ where ρ is the melt density in kg/m³. Assuming $\rho = 766$ kg/m³ for a typical PE melt, we get $\dot{\gamma} = 2.4 \times \text{MI}$. Low melt index means a high-molecular-weight, highly viscous polymer. A high melt index means low-molecular-weight, low viscosity polymer. When the melt index is less than 1, the material is said to have a fractional melt index. Such materials are used for film extrusion. Most extrusion PE grades seldom exceed MI = 12; however, for injection molding, MI is usually in the range of 5–100.

Viscosity can be measured by either capillary or rotational viscometers. In capillary viscometers, the shear stress is determined from the pressure applied by a piston. The shear rate is determined from the flow rate.

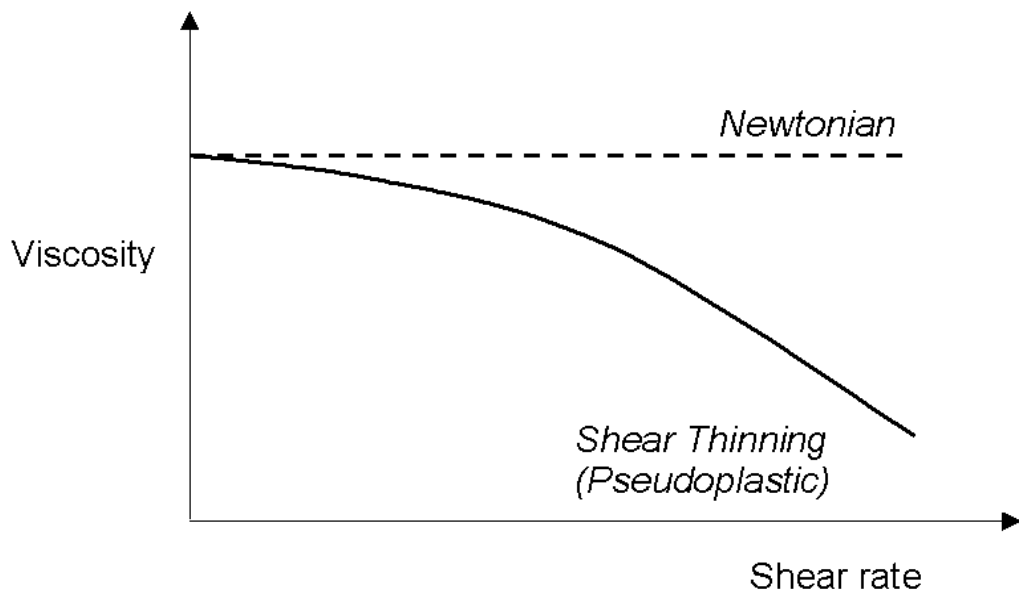


Figure 1.3. Newtonian and shear-thinning viscosity behavior.

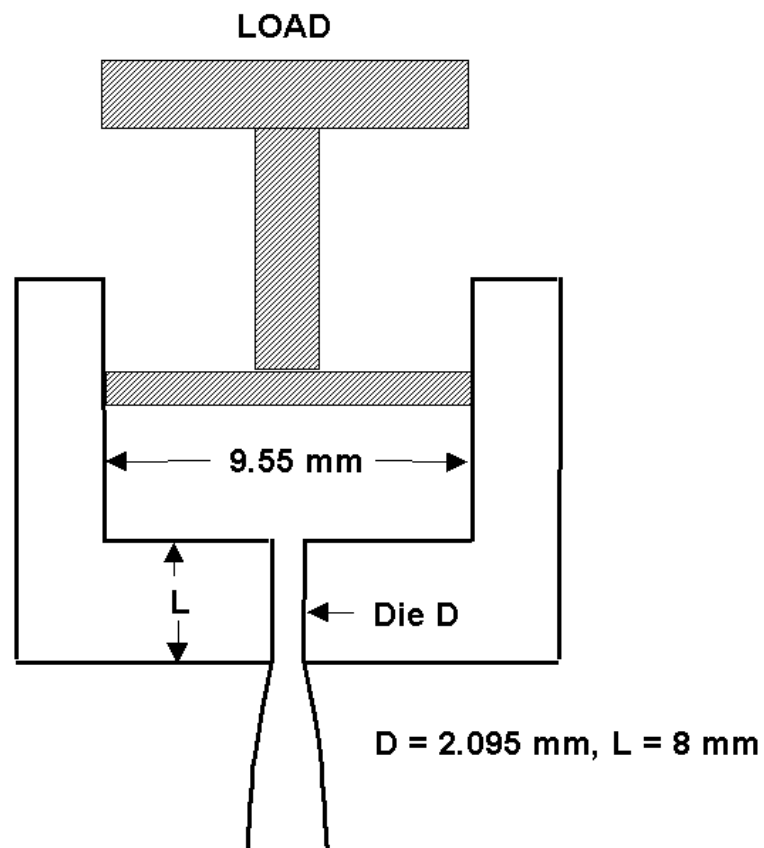


Figure 1.4. Schematic of a melt indexer.

$$\tau_w = \frac{\Delta P_{\text{cap}}}{L/R} \quad \text{shear stress} \quad (1.2)$$

$$\dot{\gamma}_a = \frac{4Q}{\pi R^3} \quad \text{apparent shear rate} \quad (1.3)$$

where ΔP_{cap} is pressure drop, L is capillary length, R is radius, and Q the volume flow rate.

The apparent shear rate corresponds to Newtonian behavior (constant viscosity fluids). A correction is necessary (Rabinowitsch correction) for shear thinning fluids. For the power-law model, the true (Rabinowitsch corrected) shear rate becomes

$$\dot{\gamma} = \frac{3n + 1}{4n} \frac{4Q}{\pi R^3} \quad (1.4)$$

This means that for a material with power-law index $n = 0.4$ (very common), the relation between apparent and true shear rate is

$$\dot{\gamma}_{\text{true}} = 1.375 \times \dot{\gamma}_{\text{apparent}} \quad (1.5)$$

When capillaries are relatively short ($L/R < 50$), the Bagley correction is necessary to account for the excess pressure drop ΔP_e at the capillary entry. The Bagley correction is usually expressed as

$$n_B = \frac{\Delta P_e}{2\tau_w} \quad (1.6)$$

where n_B may vary from 0 to perhaps 20 when polymeric materials are extruded near the critical stress for sharkskin. For a Newtonian fluid the value for n_B is 0.587.

The Bagley corrected shear stress becomes

$$\tau_w = \frac{\Delta P_{\text{cap}} + \Delta P_e}{2 \left(\frac{L}{R} + n_B \right)} \quad (1.7)$$

To apply the Bagley correction, measurements with at least two capillaries are needed.

The shear thinning behavior is frequently expressed by the power-law model

$$\eta = m \dot{\gamma}^{n-1} \quad (1.8)$$

where m is the consistency and n the power-law exponent. For $n = 1$, the Newtonian model (constant viscosity) is obtained. The smaller the value of n , the more shear-thinning the polymer. The usual range of power-law exponent values is between 0.8 (for PC) and 0.2 (for rubber compounds). For various grades of PE, the range is $0.3 < n < 0.6$. The consistency has values in the usual range of $1000 \text{ Pa}\cdot\text{s}^n$ (some PET resins) to $100,000 \text{ Pa}\cdot\text{s}^n$ for highly viscous rigid PVC. This power-law model gives a good fit of viscosity data at high shear rates but not at low shear rates (because as $\dot{\gamma}$ goes to zero, the viscosity goes to infinity).

An approximate calculation of both m and n can be carried out by using two values of the melt index (MI and HLMI). MI refers to standard weight of 2.16 kg and HLMI to “High Load” melt index (frequently 10 kg or 21.6 kg). By manipulating the appropriate equations for pressure drop, shear stress and flow rate, we have [1]:

$$\begin{aligned} \text{Power-law exponent } n &= \frac{\log(HL) - \log(LL)}{\log(HLMI) - \log(MI)} \\ \text{Consistency } m &= \frac{8982 \times (LL)}{\left[\frac{1838}{\rho} \times MI \right]^n} \end{aligned} \quad (1.9)$$

where LL is the standard load (usually 2.16 kg) and HL the high load (usually 10 kg or 21.6 kg).

Two other models are frequently used for better fitting of data over the entire shear rate range:

Carreau-Yasuda

$$\eta = \eta_o \left(1 + (\lambda \dot{\gamma})^a \right)^{\frac{n-1}{a}} \quad (1.10)$$

where η_o is the viscosity at zero shear and λ , a , and n are fitted parameters.

Cross model

$$\eta = \frac{\eta_o}{1 + (\lambda \dot{\gamma})^{1-n}} \quad (1.11)$$

where η_o is the zero shear viscosity and λ and n are fitted parameters.

With rotational viscometers (cone-and-plate or parallel plate), the shear stress is determined from the applied torque and the shear rate from the rotational speed and the gap where the fluid is sheared.

Capillary viscometers are usually used for the shear rate range from about 2 s^{-1} to perhaps 3000 s^{-1} . Rotational viscometers are usually used for the range 10^{-2} to about 5 s^{-1} . At higher rotational speeds, secondary flows and instabilities may occur which invalidate the simple

shear assumption. For more information about viscosity measurements, the reader is referred to Macosko [2].

The viscosity of polymer melts varies with temperature in an exponential manner

$$\eta = \eta_{\text{ref}} \exp(-b \Delta T) \quad (1.12)$$

The value of the temperature sensitivity coefficient b ranges from about 0.01 to 0.1 °C⁻¹. For common grades of polyolefins, we may assume that $b = 0.015$. This means that for a temperature increase $\Delta T = 10^\circ\text{C}$ (18°F), the viscosity decreases by 14%.

The effects of various factors on viscosity are summarized in Figure 1.5 following Cogswell [3]. Linear narrow molecular weight distribution polymers (e.g. metallocenes) are more viscous than their broad distribution counterparts. Fillers may increase viscosity (greatly). Pressure results in an increase in viscosity (negligible under usual extrusion conditions). Various additives are available and are designed to decrease viscosity. The zero shear viscosity increases dramatically with the weight average molecular weight:

$$\eta_o = \text{const } M_w^{3.4} \quad (1.13)$$

For some metallocene PE with long chain branching, the exponent might be much higher (perhaps 6.0).

In the above discussion of viscosity measurements, the assumption is made that the no-slip condition on the die wall is valid. This is, however, not always the case. In fact, at shear stress levels of about 0.1 MPa for PE, slip occurs. Wall slip is related to the sharkskin phenomenon [5]. Wall slip is measured by the Mooney method [6] in which the apparent shear rate ($4Q / \pi R^3$) is plotted against $1/R$ for several capillaries having different radii. In the absence of slip, the plot is horizontal. The slope of the line is equal to $4 \times$ (slip velocity).

1.2 Extensional Viscosity and Melt Strength

Extensional (or elongational) viscosity is the resistance of a fluid to extension. While it is difficult to imagine stretching of a low viscosity fluid like water, polymer melts exhibit measurable amounts of resistance. In fact, about 100 years ago, Trouton measured the resistance to stretching and shearing of stiff liquids, including pitch, and found that the ratio of extensional to shear viscosity is equal to 3.

$$\frac{\eta_e}{\eta} = 3 \quad (1.14)$$

This relation, known as the Trouton ratio, is valid for all Newtonian fluids and has a rigorous theoretical basis besides Trouton's experiments.

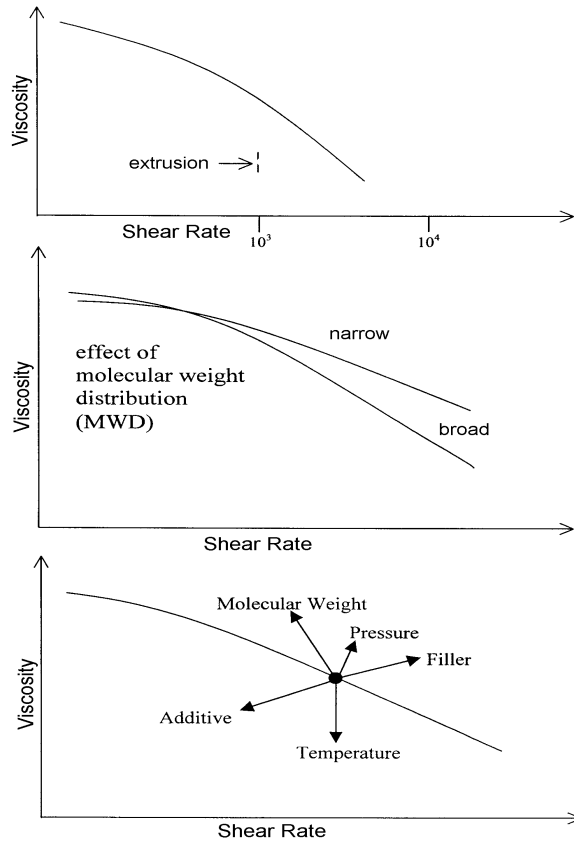


Figure 1.5. The influence of various parameters on polymer viscosity.

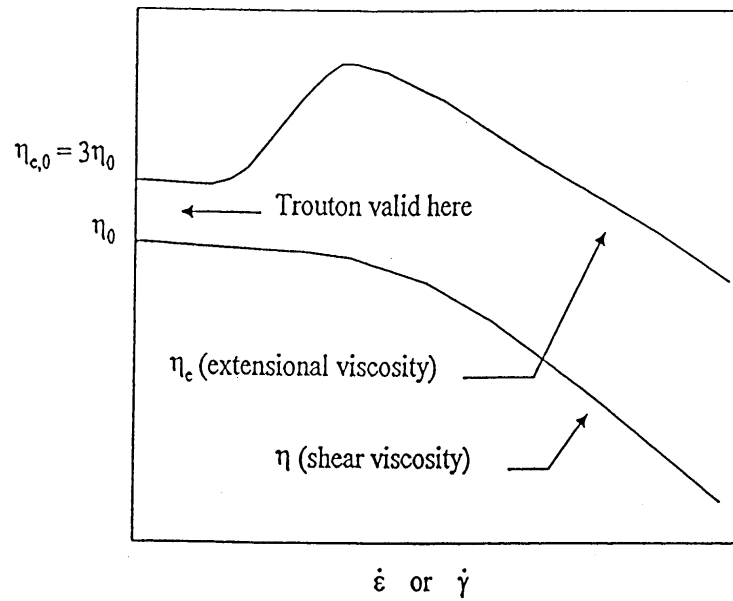


Figure 1.6. Extensional and shear viscosity as a function of stretch and shear rate, respectively.

Measurement of elongational viscosity is considerably more difficult than measurement of shear viscosity. One of the devices used involves extrusion from a capillary and subsequent stretching with the help of a pair of rollers. The maximum force required to break the extruded strand is referred to as *melt strength*. In practice, the terms extensional viscosity and melt strength are sometimes confused. Extensional viscosity is a function of the stretch rate ($\dot{\epsilon}$), as shown in Figure 1.6, and compared to the shear viscosity. Melt strength is more of an engineering measure of resistance to extension. Several extrusion processes involve extension, such as film blowing, melt spinning and sheet or film drawing. The stretch rates in film blowing can exceed 10 s^{-1} , while in entry flows from a large reservoir into a smaller diameter capillary, the maximum stretch rate is likely to be one order of magnitude lower than the maximum wall shear rate (e.g. in capillary viscometry, approximately $\dot{\epsilon}_{\text{max}} \approx 100 \text{ s}^{-1}$ for $\dot{\gamma}_{\text{max}} \approx 1000 \text{ s}^{-1}$). Frequently the extensional viscosity is plotted as a function of stretching time (increasing) without reaching a steady value (strain hardening).

The excess pressure encountered in flow from a large reservoir to a smaller diameter capillary is due to elongational viscosity. In fact, Cogswell [3] has developed a method for measurement of elongational viscosity η_e from excess pressure drop ΔP_e (i.e., the Bagley correction):

$$\eta_e = \frac{9(n+1)^2(\Delta P_e)^2}{32\eta\dot{\gamma}^2} \quad (1.15)$$

$$\text{at } \dot{\epsilon} = \frac{4\eta\dot{\gamma}^2}{3(n+1)\Delta P_e}$$

Shear and extensional viscosity measurements reveal that LLDPE (which is linear) is "stiffer" than LDPE (branched) in shear, but "softer" in extension. In extension, the linear LLDPE chains slide by without getting entangled. However, the long branches of the LDPE chains result in significantly larger resistance in extension. In the film blowing process, LDPE bubbles exhibit more stability because of their high extensional viscosity. Typical LDPE and LLDPE behavior in shear and extension is shown in Figure 1.7. LDPE is often blended with LLDPE to improve the melt strength and consequently bubble stability in film blowing. Most PP grades are known to exhibit very low melt strength. However, recent advances in polymer chemistry have led to the production of some high-melt-strength PP grades.

1.3 Normal Stresses and Extrudate Swell

Stress is defined as force divided by the area on which it acts. It has units of lb_f/in^2 (psi) in the British system or N/m^2 (Pascal, Pa) in SI. When a force is acting tangentially on a surface, the corresponding stress is referred to as *shear stress*. When a force is perpendicular (normal) to a surface, it is termed *normal stress*. Pressure is a normal stress. When a fluid is forced to flow through a conduit, it is acted upon by the normal (pressure) forces and it exerts both normal and shear (stress) forces on the conduit walls. For flow through a planar die as shown in Figure 1.2, the shear stress is zero at the midplane and maximum at the wall, while the corresponding velocity profile is quasi-parabolic. Weissenberg discovered in the 1940s that polymer solutions

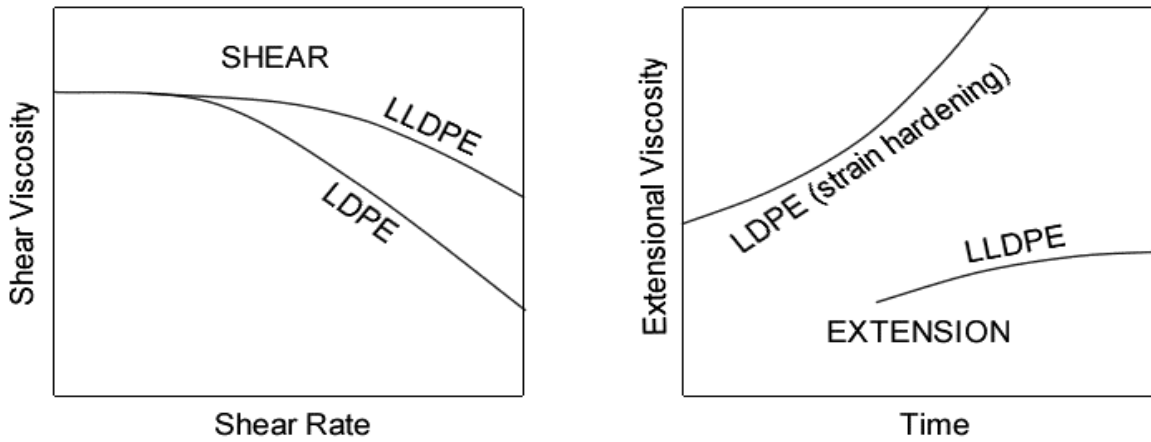


Figure 1.7. Schematic representation of LDPE and LLDPE behavior in shear and extension.

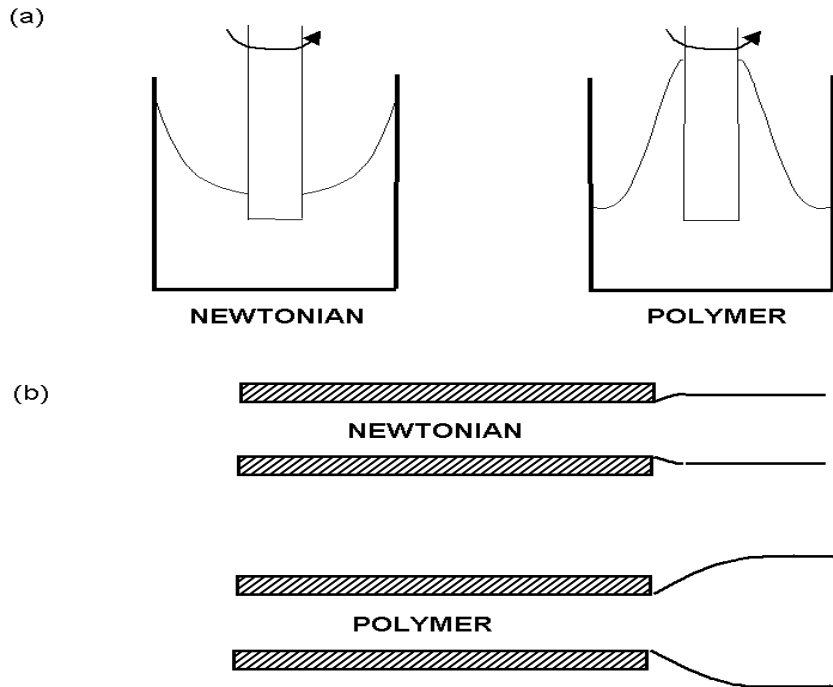


Figure 1.8. (a) Rod climbing (Weissenberg) effect in polymeric fluids, (b) extrudate swell.

and melts, when subjected to shearing, tend to develop normal stresses that are unequal in the x (direction of flow), y and z (normal directions). But, why are these elusive forces generated? Because the flow process results in anisotropies in the microstructure of the long molecular chains of polymers. Any further explanation of the physical origin of normal stresses is likely to be controversial. Here is perhaps an oversimplification: shearing means motion of a fluid in a slice-by-slice manner. If the imaginary slices were made of an extensible elastic material (like slices of rubber), shearing would also result in extension in the flow direction and uneven compression in the other two directions. So, when an (elastic) polymer solution or melt is forced to flow, it is less compressed in the direction of flow than in the other two normal directions.

The so-called First Normal Stress Difference N_1 is defined as the normal stress in the direction of the flow (τ_{xx}) minus the perpendicular (τ_{yy})

$$N_1 = \tau_{xx} - \tau_{yy} \quad (1.16)$$

The Second Normal Stress Difference is

$$N_2 = \tau_{yy} - \tau_{zz} \quad (1.17)$$

Experiments show that N_1 is positive for usual polymers (i.e. extensive, while the compressive pressure forces are negative). N_2 is negative and of the order of 20% of N_1 for most common polymers.

The normal stress differences can be very large in high-shear-rate extrusion. Some authors suggest a variation for the normal stress difference at the wall in the form

$$N_{1w} = A \tau_w^b \quad (1.18)$$

The stress ratio

$$S_R = \frac{N_{1w}}{2 \tau_w} \quad (1.19)$$

can reach a value of 10 or more at the onset of melt fracture.

The rod-climbing (Weissenberg) effect observed (Figure 1.8 (a)) when a cylinder rotates in a polymeric liquid is due to some sort of "strangulation" force exerted by the extended polymer chains, which results in an upward movement normal to the direction of rotation (normal stress difference). The extrudate swell phenomenon [7] (see Figure 1.8 (b)) is due mainly to the contraction of exiting polymer that is under extension in the die. The uneven compression in the various directions results in a number of unusual flow patterns and instabilities. The secondary flow patterns observed by Dooley and co-workers [8] are due to the second normal stress difference. Bird *et al.* [9] in their book state: "A fluid that's macromolecular is really quite weird, in particular the big normal stresses the fluid possesses give rise to effects quite spectacular."

The phenomenon of extrudate swell (also known as die swell) has been studied by several researchers. While the primary mechanism is release of normal stresses at the exit, other effects are also important. The amount of swell is largest for zero length dies (i.e. orifices). It decreases for the same throughput with the length of the die due to fading memory as the residence time in the die increases. Even Newtonian fluids exhibit some swell upon exiting dies (13% for round extrudates, 19% for planar extrudates). This is due to streamline rearrangement at the exit. The amount of swell can be influenced by thermal effects due to viscosity differences between the walls and center of a die. Maximum thermal swell can be obtained when a hot polymer flows through a die having colder walls. Swell ratio of about 5% on top of other mechanisms can be obtained from temperature differences.

Several attempts have been made to predict extrudate swell numerically through equations relating the swell ratio d/D (extrudate diameter / die diameter) to the first normal stress difference at the wall N_{1w} . Based on the theory of rubber elasticity, the following is obtained [7]

$$N_{1w} = 2\tau_w \left(3 \left[\left(\frac{d}{D} \right)^4 + 2 \left(\frac{d}{D} \right)^{-2} - 3 \right] \right)^{1/2} \quad (1.20)$$

Based on stress release for a Maxwell fluid exiting from a die, Tanner's equation applies [7]

$$N_{1w} = 2\sqrt{2}\tau_w \left[\left(\frac{d}{D} - 0.13 \right)^6 - 1 \right]^{1/2} \quad (1.21)$$

Although *Equation 1.21* has a more rigorous derivation and theoretical basis, the rubber elasticity theory (*Equation 1.20*) gives better predictions.

1.4 Stress Relaxation and Dynamic Measurements

After cessation of flow, the stresses become immediately zero for small molecule (Newtonian) fluids like water or glycerin. For polymer melts, the stresses decay exponentially after cessation of flow. Stress relaxation can be measured in a parallel plate or a cone-and-plate rheometer by applying a given shear rate level (rotation speed/gap) and measuring the stress decay after the rotation is brought to an abrupt stop. Such tests, however, are not performed routinely because of experimental limitations.

Dynamic measurements involve the response of a material to an imposed sinusoidal stress or strain on a parallel plate or cone-and-plate instrument. A perfectly elastic material that behaves like a steel spring, by imposition of extension (strain), would develop stresses that would be in-phase with the strain, because

$$\text{stress}(\tau) = \text{modulus}(G) \times \text{strain}(\gamma) \quad (1.22)$$

However, for a Newtonian fluid subjected to a sinusoidal strain, the stress and strain will not be in-phase because of the time derivative (strain rate) involved

$$\tau = \eta \dot{\gamma} \quad (1.23)$$

$$\begin{aligned} &= \eta \frac{d\gamma}{dt} = \eta \frac{d}{dt}(\gamma_o \sin \omega t) = \eta \omega \gamma_o \cos \omega t \\ &= \eta \omega \gamma_o \sin(\omega t + 90^\circ) \end{aligned} \quad (1.24)$$

where ω is frequency of oscillation. That is, a Newtonian fluid would exhibit 90° phase difference between stress and strain. Polymeric liquids that are partly viscous and partly elastic (viscoelastic) will be $0 \leq \phi \leq 90^\circ$ out of phase.

We can define

$$G'(\omega) = \frac{\text{in - phase stress}}{\text{maximum strain}} \quad \begin{array}{l} \text{storage} \\ \text{modulus} \\ \text{(elastic part)} \end{array} \quad (1.25)$$

$$G''(\omega) = \frac{\text{out - of - phase stress}}{\text{maximum strain}} \quad \begin{array}{l} \text{loss} \\ \text{modulus} \\ \text{(viscous part)} \end{array} \quad (1.26)$$

where ω ranges usually from 0.01 to 10^3 rad/s. Larger G' implies more elasticity. Further, we can define

$$\eta' = \frac{G''}{\omega} \quad \text{the dynamic viscosity} \quad (1.27)$$

$$\eta'' = \frac{G'}{\omega} \quad (1.28)$$

and the magnitude of the complex viscosity

$$|\eta^*| = (\eta'^2 + \eta''^2)^{1/2} \quad (1.29)$$

An empirical relationship called the "Cox-Merz rule" states that the shear rate dependence of the steady state viscosity η is equal to the frequency dependence of the complex viscosity η^* , that is

$$\eta(\dot{\gamma}) = |\eta^*(\omega)| \quad (1.30)$$

The usefulness of this rule, which holds for most polymers, is that while steady measurements of shear viscosity are virtually impossible above 5 s^{-1} with rotational instruments, the dynamic measurements can easily be carried out up to 500 rad/s (corresponds to $\dot{\gamma} = 500 \text{ s}^{-1}$) or even higher. Thus, the full range of viscosity needed in extrusion can be covered.

Some typical results involving narrow and broad molecular-weight-distribution samples are shown in Figure 1.9. The relative behavior of G' versus ω can be used to identify whether a sample is of narrow or broad molecular weight distribution [6]. In fact, from the "crossover point" where $G' = G''$, it is possible to get a surprisingly good estimate of the polydispersity M_w/M_n for PP [10].

1.5 Constitutive Equations

These are relations between stresses and strains (deformations). In its simplest form, the Newtonian equation is

$$\tau = \eta \dot{\gamma}_{\text{fluid}} \quad (1.31)$$

where η is viscosity and $\dot{\gamma} = du/dy$, the shear rate.

For a shear thinning material of the power-law type, we have

$$\tau = \eta \dot{\gamma} = m \dot{\gamma}^{n-1} \cdot \dot{\gamma} = m \dot{\gamma}^n \quad (1.32)$$

where m is consistency and n the power-law exponent.

However, the above expressions, when inserted into the equation of conservation of momentum, cannot predict viscoelastic effects such as normal stresses, stress relaxation or extrudate swell. The simplest way to develop viscoelastic constitutive equations is to combine a model for an elastic solid

$$\tau = \mathbf{G} \gamma_{\text{solid}} \quad (1.33)$$

with that for a Newtonian fluid

$$\tau = \eta \dot{\gamma}_{\text{fluid}} \quad (1.34)$$

By differentiating *Equation 1.33* and adding the two strain rates, we get

$$\frac{\dot{\tau}}{\mathbf{G}} + \frac{\tau}{\eta} = \dot{\gamma} \quad (1.35)$$

or

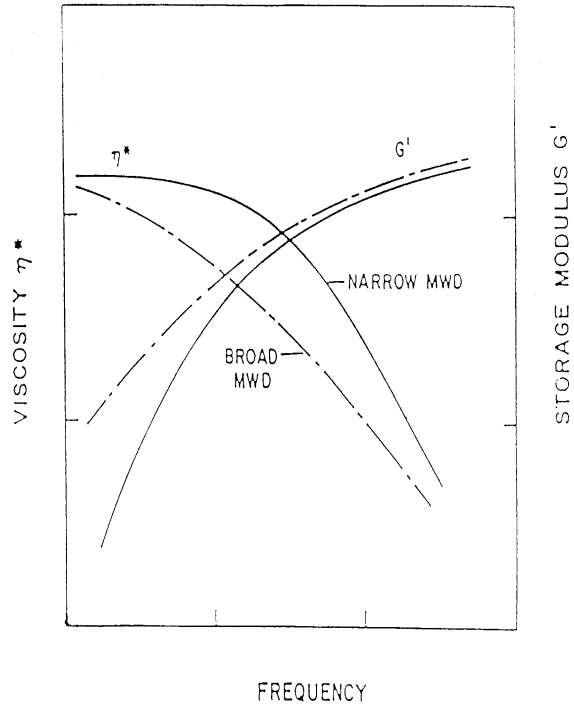


Figure 1.9. Storage modulus G' and dynamic viscosity η^* behavior of broad and narrow molecular weight distribution polymers.

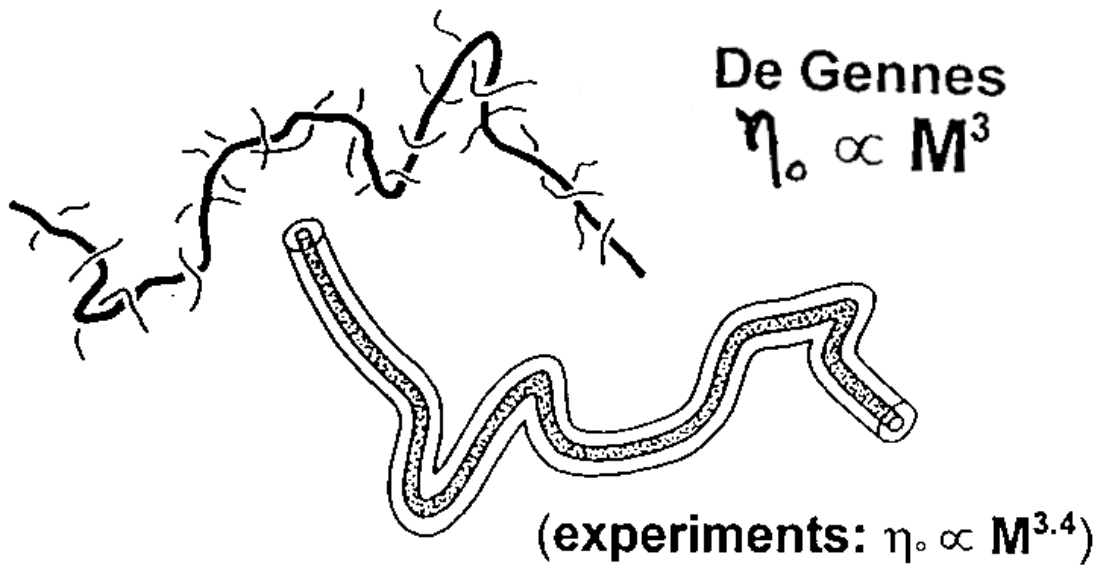


Figure 1.10. Reptation model of polymer chain motion.

$$\tau + \frac{\eta}{G} \dot{\tau} = \eta \dot{\gamma} \quad (1.36)$$

$\frac{\eta}{G} = \lambda$ has dimensions of time (relaxation constant).

$$\tau + \lambda \dot{\tau} = \eta \dot{\gamma} \quad (1.37)$$

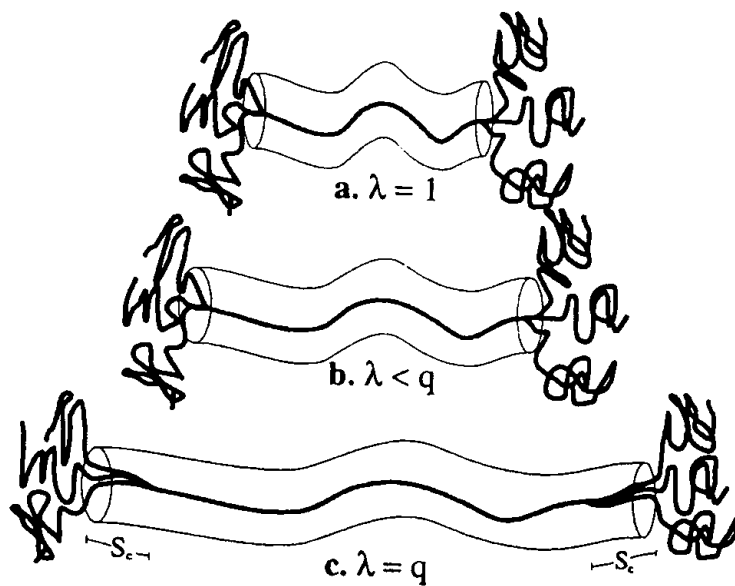
This is known as the Maxwell model. Viscoelastic models must be expressed in three dimensions and in a proper mathematical frame of reference that moves and deforms with the fluid. The result is a very complicated expression involving dozens of derivatives [11,12].

The most powerful constitutive equation is the so-called K-BKZ integral model that involves more than two dozen experimentally fitted parameters (see, for example: Mitsoulis [13]). Current trends involve the development of models based on macromolecular motions. De Gennes proposed the snake-like motion of polymer chains called reptation, illustrated in Figure 1.10. Based on the reptation concept, Doi and Edwards [2] developed a constitutive equation which leaves much to be desired before it can be used for prediction of viscoelastic flow phenomena. Several attempts have been made to fix the Doi-Edwards theory. The most prominent researcher in the area is G. Marrucci (see, for example: Marrucci and Ianniruberto [14]).

The most talked about viscoelastic model recently is the Pom-Pom polymer model, developed by T.C.B. McLeish and R.G. Larson [15]. The motivation for its development was that the K-BKZ equation fails to predict the observed degree of strain hardening in planar extension when the kernel functions are adjusted to fit the observed degree of strain softening in shear. The failure to describe the rheology of long-chain branched polymers suggests that some new molecular insight is needed into the nonlinear relaxation processes that occur in such melts under flow. The Pom-Pom model uses an H-polymer structure, in which molecules contain just two branch points of chosen functionality – a “backbone” which links two pom-poms of q arms each, as shown in Figure 1.11.

The Pom-Pom model exhibits rheological behavior remarkably similar to that of branched commercial melts like LDPE. It shows strain hardening in extension and strain softening in shear. It can describe both planar and uniaxial extension. The constitutive equation is integro-differential. For successful application at least 32 parameters must be obtained by fitting experimental rheological data. Of course, best fitting 32 or more parameters of a complicated constitutive equation is a mathematical challenge of its own.

Modeling of the viscoelastic behavior of polymers has always been a very controversial subject. The viscoelastic constitutive equations have contributed towards the understanding of the various mechanisms of deformation and flow, but unfortunately have not provided us with quantitative predictive power. Very often the predictions depend on the model used for the computations and are not corroborated with experimental observations. Some viscoelastic flow problems can be solved with the appropriate constitutive equations, but this is still an area of academic research with limited practical applications at the moment.



The structure of a pom-pom polymer with a backbone and $2q$ dangling arms, with $q = 3$, under various degrees of stretch. The stretch of the backbone is denoted by the variable $\lambda(t)$, the path length of arm withdrawn into the backbone tube by the variable $s_c(t)$.

Figure 1.11. Pom-Pom polymer model idealized molecules.

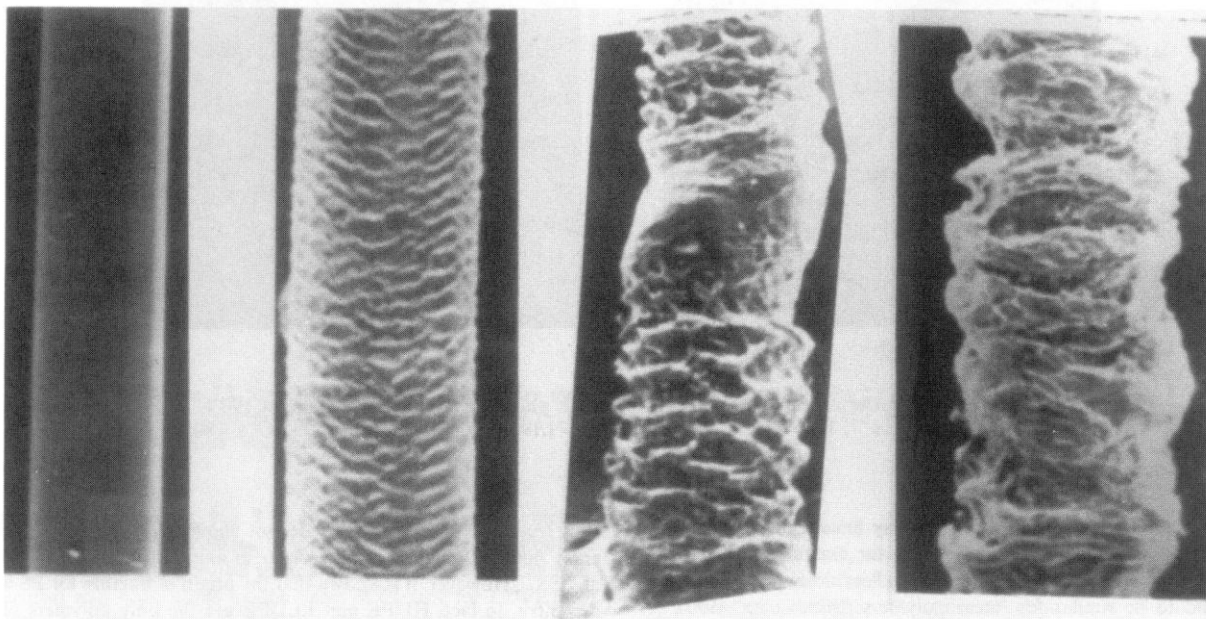


Figure 1.12. LLDPE extrudates obtained from a capillary at apparent shear rates of 37, 112, 750 and 2250 s^{-1} .

1.6 Sharkskin, Melt Fracture and Die Lip Build-Up

The term *sharkskin* refers to the phenomenon of loss of surface gloss of an extrudate, also sometimes termed surface mattness. The surface usually exhibits a repetitious wavy or ridged pattern perpendicular to the flow direction. It occurs at a critical stress level of at least 0.14 MPa (21 psi) for most common polymers extruded through capillary dies. With some additives, lubricants, processing aids or die coatings, the onset of sharkskin can be shifted to a higher shear stress level, with values up to 0.5 MPa being reported.

The prevailing point of view is that sharkskin originates near the die exit and is due to stick-slip phenomena. A critical shear stress near the exit in conjunction with a critical acceleration results in skin rupture of the extrudate [16,17]. There was some disagreement over whether slip between the polymer and the die wall causes or helps avoid sharkskin [18]. However, it is now believed that it is slip which helps to postpone sharkskin to higher flow rates. Good adherence is also thought to be potentially beneficial, but stick-slip is always detrimental.

Minute amounts of (expensive) fluorocarbon polymers are used as processing aids with LLDPE. The proposed mechanism is that they deposit on the die surface and allow continuous slip. More recently boron nitride has been introduced for the same purpose [19]. Other remedies for postponing the onset of sharkskin to higher throughput rates involve reducing the wall shear stress by heating the die lips to reduce the polymer viscosity and by modifying the die exit to include a small exit angle (flaring).

At higher throughput rates, extrudates usually become highly distorted and the pressure in a capillary viscometer shows significant fluctuations. This phenomenon is known as gross melt fracture.

Figure 1.12 shows LLDPE extrudates for increasing shear rates, illustrating the progression from smooth surface to sharkskin and then melt fracture [20]. It is possible with some polymers to obtain melt fractured extrudates without sharkskin, i.e. the surface remains smooth and glossy but overall the extrudate is distorted.

Proposed mechanisms for melt fracture include entry flow vortex instability, elastic instability during flow in the die land for stress ratios greater than about 10 (see *Equation 1.19*), stick-slip phenomena and other interactions between the polymer and the metal die wall. Probably more than one mechanism is responsible.

Die lip build-up (also known as die drool) refers to the gradual formation of an initially liquid deposit at the edge of the die exit which solidifies and grows and may partially obstruct the flow of the extruded product and/or cause defective extrudate surface. Depending on the severity of the problem, continuous extrusion must be interrupted every few hours or days and the solid deposit removed from the die lips. The causative mechanisms are not really known. Observations suggest that the formation of die lip build-up is not continuous but intermittent. Tiny droplets of material come out of the die or perhaps from a rupturing extrudate surface. Some studies suggest that the build-up is rich in lower molecular weight polymer fractions, waxes and other additives [21].

Remedies for reducing die lip build-up include repairing missing plating and surface imperfections from die lips, removing moisture from the feed material, lowering the extrudate temperature and adding stabilizer to the resin. Fluorocarbon processing aids will sometimes also be helpful, as they are with sharkskin. The melt fracture remedy of small die exit angles (flaring) is also known to reduce build-up, for polyethylenes and polycarbonate.

1.7 Rheological Problems in Coextrusion

1.7.1 Layer-To-Layer Non-Uniformity

Layer non-uniformity in coextrusion flows is caused mainly by the tendency of the less viscous polymer to go to the region of high shear (i.e. the wall) thereby producing encapsulation. Figure 1.13 illustrates this phenomenon for rod and slit dies [22]. Complete encapsulation is possible for extremely long dies (this is not encountered in coextrusion practice). Differences in wall adhesion and viscoelastic characteristics of polymers are also contributing factors. Weak secondary flows caused by viscoelastic effects (from the second normal stress difference) have been demonstrated to produce layer non-uniformities even in coextrusion of different colored streams of the same polymer [23]. Reduction of this defect can be achieved by choosing materials with the smallest possible differences in viscosity and viscoelasticity (G' , G'' , extrudate swell), or by changing the stream temperatures to bring the polymer viscosities closer to one another.

Layer non-uniformity can also arise in feedblock cast film coextrusion, in which melt streams are merged into a single stream in a feedblock prior to entering the flat die for forming. Uneven flow leakage from the flat die manifold to the downstream sections of the die can lead to encapsulation of the more viscous polymer by the less viscous, or even the reverse! The technique of feedblock profiling is used to counteract the natural tendency for encapsulation from viscosity differences. This involves contouring the feedblock flow passages for regions of high or low volumetric throughput, as shown in Figure 1.14. Feedblock profiling combined with elimination of uneven flow leakage from the feeding section of a flat die (or the use of this leakage to counteract the natural tendency for encapsulation) can be used to produce layer-to-layer uniformity in the extrudate. The problem is much more complex in coextrusion of many layers, as profiling for one layer will disrupt the other layers. The influence of a feedblock design change is virtually impossible to predict at present, even with the use of the most powerful 3-D finite element flow simulation packages on powerful supercomputers.

1.7.2 Interfacial Instability

Interfacial instability in coextrusion refers to two common types of defects consisting of highly irregular or sometimes regular waviness which appears in coextruded structures at the polymer/polymer interface. The effect is to significantly reduce the optical quality of coextruded film. It is an internal defect, which distinguishes it from sharkskin, which is a surface defect.

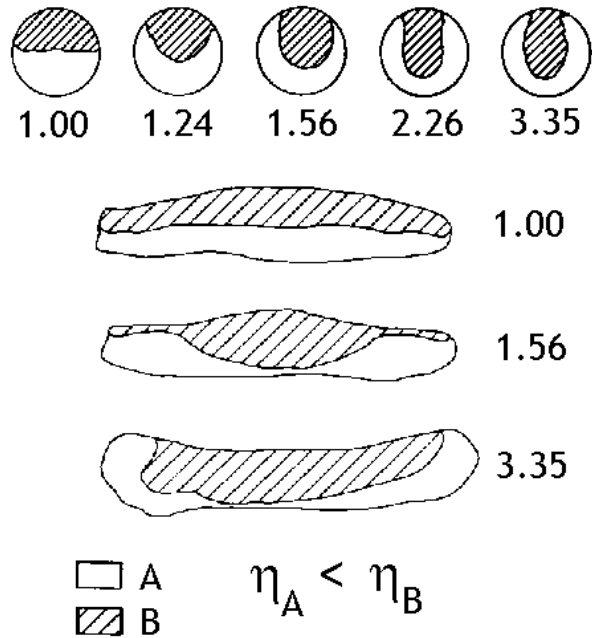


Figure 1.13. Layer-to-layer flow rearrangement as a function of time.

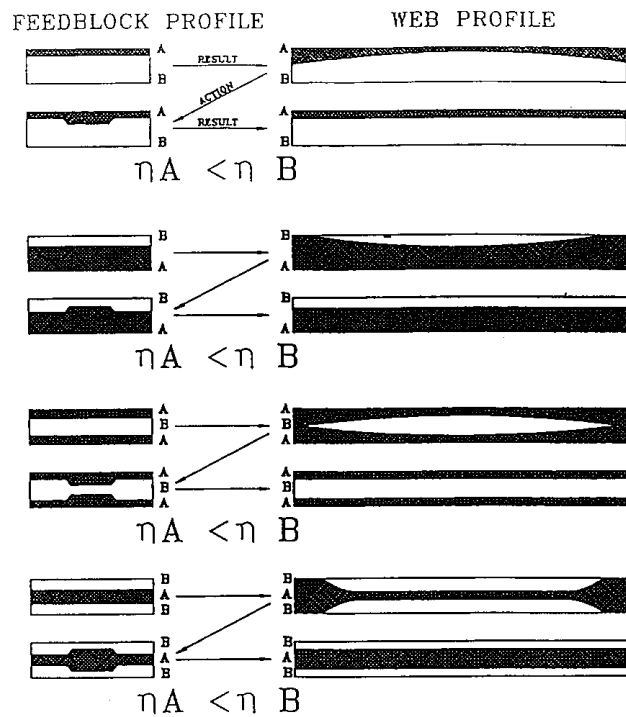


Figure 1.14. Feedback profiling and the resultant effects.

The most frequently encountered type of interfacial instability is zig-zag (also known as die-land) instability, which appears as chevrons pointing in the flow direction. It is initiated in the die land and is characterized by a critical interfacial shear stress, in the range of 30 kPa to 80 kPa (roughly $\frac{1}{4}$ to $\frac{1}{2}$ of the critical wall shear stress level for sharkskin). Figure 1.15 shows the effect of this instability on film clarity [24]. This problem can arise even if adjacent layers are of the same material. The mechanism responsible has not been conclusively identified. Apparently there is amplification of certain disturbance wavelengths under high stress conditions [25]. Viscoelasticity is probably a contributing factor, i.e. the value of interfacial normal stress difference is important. Unfortunately this is impossible to measure and difficult to calculate accurately. The most reliable means of diagnosing zig-zag instability at present is to calculate interfacial shear stress using simulation software.

Zig-zag instability problems are remedied by reducing interfacial shear stresses. The following actions are beneficial:

- decrease the total output rate (this reduces stresses everywhere)
- increase the skin layer thickness (this will shift the interface away from the wall where the shear stress is maximum)
- decrease the viscosity of the skin layer, i.e. by raising its temperature or by using a less viscous polymer (this reduces stresses everywhere)
- increase the die gap (this reduces stresses everywhere)

Viscosity matching of layers is a popular remedy that does NOT always work. In fact, as recommended above, it is often advisable to intentionally mismatch the viscosities by using a low viscosity resin for the skin layer.

The less common type of interfacial instability is “wave” pattern instability, which appears as a train of parabolas spanning the width of the sheet and oriented in the flow direction. It occurs when a fast moving polymer stream merges with a much slower moving stream in a coextrusion feedblock. When the skin layer is thin relative to the second layer (i.e. the skew of the coextruded structure is small), the wave instability can be more pronounced. Large differences in extensional viscosities between adjacent layers can also make the defect more likely, as can large extensional viscosity of the skin layer. The instability is aggravated by whatever flow or geometrical asymmetries might be present in the feedblock and die. As well, dies with larger lateral expansion ratios (die lip width divided by manifold entry width) and longer channel lengths (from feed slot vanes to die manifold) are more susceptible [26].

1.8 Troubleshooting With the Help of Rheology

Rheological measurements (viscosity, elongational viscosity, G' and G'') can be used for (a) material characterization, (b) determination of processability, and (c) as input data for computer simulations [1].

In material characterization, rheology has an advantage over other methods because of its sensitivity to certain aspects of the structure such as the high molecular weight tail and branching. Also, in many instances, rheological characterization can be a lot faster than other methods such as GPC.

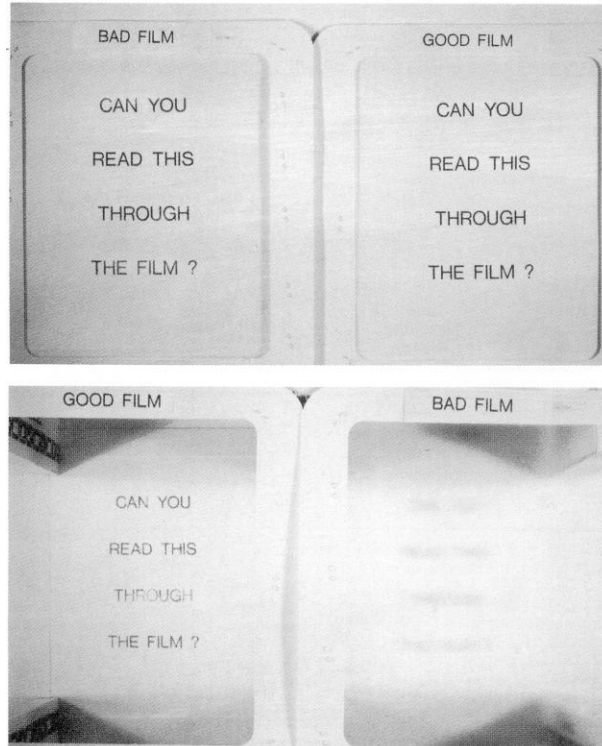


Figure 1.15. The effect of interfacial instability on contact clarity of coextruded films (top) versus see-through clarity (bottom).

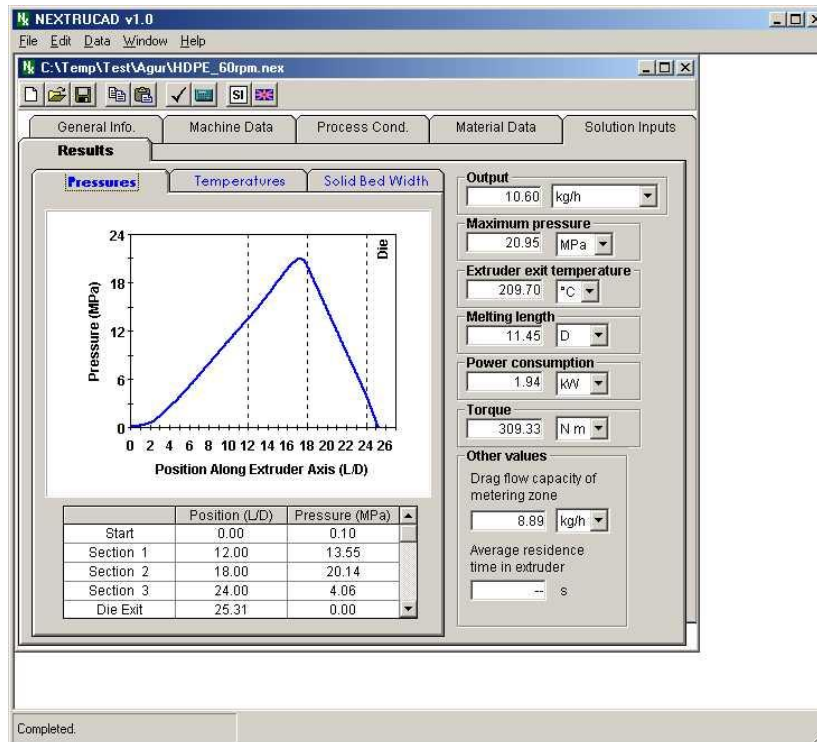


Figure 1.16. Simulation prediction of pressure build-up in extruder.

With careful rheological measurements, it is possible to determine whether, or under what conditions, a material will be processable. Blend ratios, or additive quantities necessary to facilitate processing can be determined. Many problems can be avoided by a thorough rheological characterization, before the material is introduced into the extruder hopper. For the relative benefits of on-line, in-line or off-line rheometry, the reader is referred to Kelly *et al.* [27].

Rheological measurements are absolutely necessary as input for computer simulations. The viscosity must be measured over the shear rate range that is anticipated in the real process, and then fitted to a proper model (power-law, Carreau-Yasuda or Cross). Figure 1.16 shows a prediction of pressure build-up in an extruder made using viscosity data [28]. Other measurements are necessary, whenever viscoelastic simulations are undertaken.

Rheology is used for troubleshooting purposes in a great variety of situations. Here are some frequently encountered ones:

Processability of material A versus material B. A frequently asked question from rheology consultants is: "Materials A and B have the same Melt Index (MI), virtually identical viscosity curves and virtually identical molecular weight distributions (measured by Gel Permeation Chromatography (GPC)). Yet, they behave very differently in extrusion through the same machine. Why?" The reason is that processability is often determined by small amounts of high molecular weight fractions or branching which are not detectable by conventional GPC methods and do not cause any measurable differences in MI or the viscosity curve. To detect the differences it is recommended that G' and G'' be determined and compared. Occasionally, first normal stress difference measurements (N_1) might be necessary, and since these are difficult and expensive, extrudate swell measurements are recommended. Larger G' , N_1 or extrudate swell implies the presence of a higher-molecular-weight tail. For processing involving extension (blown film, melt spinning, sheet and film drawing), measurements of extensional viscosity (or melt strength) are recommended.

Final product properties are poor. These may include impact resistance, optics, warpage, brittleness, etc. Again, rheological measurements may have to be carried out on samples from the raw material and from the final product for comparison purposes. This is aimed at detecting any degradation or other modification that might have occurred during extrusion.

Material is prone to sharkskin. Determine the viscosity of material at the processing temperature (in the lip region). Materials that are not very shear thinning are prone to sharkskin at relatively low throughput rates. To reduce shear stress, increase die temperature or use additives that promote slippage (e.g. fluorocarbon polymers).

Bubble instability in film blowing. One of the causes might be low melt strength of the material. Measure extensional viscosity and/or melt strength. Compare with other materials that show better bubble stability. Choose a higher melt strength material. Increase cooling to lower bubble temperature and thereby increase melt strength.

Draw resonance in melt spinning or drawing of cast film. Draw resonance refers to periodic diameter or thickness variation. Low-elasticity materials are more prone to this type of instability. Measure G' and choose more elastic resin grades (higher G').

Poor blending of two polymers. When the viscosity difference between two polymers to be blended is large (say, over five times), blending is difficult because the shear stress exerted by the matrix on the higher viscosity dispersed phase is not large enough to cause breakup. Use a matrix of higher viscosity or an extensional flow mixer [1].

1.9 Concluding Remarks

Polymer resins are frequently sold on the basis of density and Melt Index (MI). However, MI is only just one point on an (apparent) viscosity curve. Plastics extrusion involves shear rates usually up to 1000 s^{-1} , and viscosity measurements are called for to determine the shear thinning behavior. For the analysis of some processes, knowledge of extensional viscosity and/or melt strength may be needed. The level of elasticity is indicated by the normal stress differences and dynamic modulus measurements (G' and G'').

Rheology is an excellent tool for materials characterization and miscellaneous troubleshooting purposes. However, understanding of the problem is absolutely necessary for the successful application of rheological methods for pinpointing the root causes of various extrusion defects.

1.10 References

1. J. Vlachopoulos and J.R. Wagner (eds.), *The SPE Guide on Extrusion Technology and Troubleshooting*, Society of Plastics Engineers, Brookfield CT (2001).
2. C.W. Macosko, *Rheology: Principles, Measurements and Applications*, VCH Publishers, New York (1994).
3. F.N. Cogswell, *Polymer Melt Rheology*, Woodhead Publishing, Cambridge, England (1996).
4. A.V. Chenoy and D.R. Saini, *Thermoplastic Melt Rheology and Processing*, Marcel Dekker, New York (1996).
5. S.G. Hatzikiriakos, *Polym. Eng. Sci.*, **34**, 1441 (1994).
6. J.M. Dealy and K.F. Wissbrun, *Melt Rheology and Its Role in Plastics Processing*, Chapman and Hall, London (1996).
7. J. Vlachopoulos, *Rev. Def. Beh. Mat.*, **3**, 219 (1981).
8. B. Debbaut, T. Avalosse, J. Dooley, and K. Hughes, *J. Non-Newt. Fluid Mech.*, **69**, 255 (1997).
9. R.B. Bird, R.C. Armstrong, and O. Hassager, *Dynamics of Polymeric Liquids*, Vol. I, Wiley, New York (1987).
10. S.W. Shang, *Adv. Polym. Tech.*, **12**, 389 (1993).
11. R.I. Tanner, *Engineering Rheology*, Oxford Engineering Science, Oxford, England (2000).
12. D.G. Baird and D.J. Collias, *Polymer Processing Principles and Design*, Wiley, New York (1998).
13. E. Mitsoulis, *J. Non-Newt. Fluid Mech.*, **97**, 13 (2001).
14. G. Marrucci and G. Ianniruberto, *J. Rheol.*, **47**, 247 (2003).
15. T.C.B. McLeish and R.G. Larson, *J. Rheol.*, **42**, 81 (1998).
16. R. Rutgers and M. Mackley, *J. Rheol.*, **44**, 1319 (2000).
17. M.M. Denn, *Ann. Rev. Fluid Mech.*, **33**, 265 (2001).
18. A.V. Ramamurthy, *Proceedings of Xth Intl. Cong. Rheo.*, Sydney (1988).
19. E.C. Achilleos, G. Georgiou and S.G. Hatzikiriakos, *J. Vinyl Addit. Techn.*, **8**, 7 (2002).
20. R. H. Moynihan, PhD thesis, Dept. of Chem. Eng., Virginia Tech. (1990).
21. J.D. Gander and J. Giacomini, *Polym. Eng. Sci.*, **37**, 1113 (1997).
22. N. Minagawa and J.L. White, *Polym. Eng. Sci.*, **15**, 825 (1975).
23. J. Dooley, PhD thesis, U. Eindhoven, Netherlands (2002).
24. R. Shroff and H. Mavridis, *Plas. Tech.*, 54 (1991).
25. J. Perdikoulis and C. Tzoganakis, *Plas. Eng.*, **52**, #4, 41 (1996).
26. R. Ramanathan, R. Shanker, T. Rehg, S. Jons, D.L. Headley and W.J. Schrenk, *SPE ANTEC Tech. Papers*, **42**, 224 (1996).
27. A.L. Kelly, M. Woodhead, R.M. Rose, and P.D. Coates, *SPE ANTEC Tech. Papers*, **45**, 1979 (1999).
28. NEXTRUCAD, Polydynamics, Inc., <http://www.polydynamics.com>.